

Lab on a Chip

Accepted Manuscript



This is an *Accepted Manuscript*, which has been through the Royal Society of Chemistry peer review process and has been accepted for publication.

Accepted Manuscripts are published online shortly after acceptance, before technical editing, formatting and proof reading. Using this free service, authors can make their results available to the community, in citable form, before we publish the edited article. We will replace this *Accepted Manuscript* with the edited and formatted *Advance Article* as soon as it is available.

You can find more information about *Accepted Manuscripts* in the [Information for Authors](#).

Please note that technical editing may introduce minor changes to the text and/or graphics, which may alter content. The journal's standard [Terms & Conditions](#) and the [Ethical guidelines](#) still apply. In no event shall the Royal Society of Chemistry be held responsible for any errors or omissions in this *Accepted Manuscript* or any consequences arising from the use of any information it contains.

Fabrication of 3D High Aspect Ratio PDMS Microfluidic Networks with a Hybrid Stamp

Yu-Chun Kung^a, Kuo-Wei Huang^a, Yu-Jui Fan^{ab}, and Pei-Yu Chiou^{a*}

^a Mechanical and Aerospace Engineering Department, University of California, Los Angeles, USA

^b Institute of Applied Mechanics, National Taiwan University, Taipei, TAIWAN

Abstract

We report on a novel methodology for fabricating large-area, multilayer, thin-film, high aspect ratio, 3D microfluidic structures with through-layer vias and open channels that can be bonded between hard substrates. It is realized by utilizing a hybrid stamp with a thin plastic sheet embedded underneath a PDMS surface. This hybrid stamp solves an important edge protrusion issue during PDMS molding process while maintaining necessary stamp elasticity to ensure the removal of PDMS residues at through-layer regions. Removing edge protrusion is a significant progress toward fabricating 3D structures since high aspect ratio PDMS structures with flat interfaces can be realized to facilitate multilayer stacking and bonding with hard substrates. Our method also allows for the fabrication of 3D deformable channels, which can lead to profound applications in electrokinetics, optofluidics, inertial microfluidics, and other fields where the shape of channel cross-section plays a key role in device physics. To demonstrate, as an example, we have fabricated a microfluidic channel by sandwiching two 20 μm wide, 80 μm tall PDMS membranes between two featureless ITO glass substrates. By applying an electrical bias to the two ITO substrates and a pressure to deform the thin membrane sidewalls, strong electric field enhancement can be generated in the center of a channel to enable 3D sheathless dielectrophoretic focusing of biological objects including mammalian cells and bacteria at a flow speed up to 14 cm/sec.

Introduction

Lab on a chip systems have attracted tremendous interests in both academics and industries in the past decade for their potential applications in personal medicine, health care, environmental monitoring, and chemical synthesis [1]. With the increasing demand of more integrated functions on a chip, advancements in manufacturing technology are critical to provide flexibility on integration of heterogeneous materials, a better interface between macro and micro components, and simple routing approaches for massively parallel fluid manipulation and control. 3D microfluidics is one of the future trends since it not only significantly increases the number of functional units that can be integrated on a chip, thus increasing the processing power and throughput, but also provides many important unique functions that are difficult to realize with conventional 2D technologies [2-4], such as 3D sheath flows for sample focusing [5, 6] and 3D tissue engineering[7-14].

Versatile approaches have been demonstrated in prior literatures for fabricating 3D microfluidic structures. Silicon-based microfabrication allows the creation of high-resolution, high aspect ratio structures on silicon substrates, high conductivity metal electrodes for electrical sensing and actuation, and high quality semiconductor devices for IC integration. The drawbacks, however, are the high manufacturing costs and challenges to integrate with other microfluidic components. Thermal plastic hot embossing is a fast and efficient way for fabricating microfluidic structures[15]. Yet, it has residual membrane issues and cannot be used to fabricate uniform through-layer structures for interlayer communication. Photosensitive epoxy polymers such as SU-8 can be optically patterned and stacked through thermal bonding [16-18]. However, it is well known that during the spin-coating process, uneven thickness around the structures can hinder uniform bonding across a large area, which potentially leads to fluid leak.

Multilayer soft lithography (MSL) has been widely applied for fabricating microfluidic devices in the recent decade [19]. Numerous PDMS based devices from simple monolayer PDMS channels to complex multilayer microfluidic systems with pneumatically controlled pumps and valves have been demonstrated [20]. Thousands of valves and chambers can be integrated on a chip to perform multistep biochemical analyses [21]. Most PDMS based devices, however, are not true 3D devices since they do not have through-layer structures such as holes or channels for vertical fluid routing. This limitation comes from the lack of a reliable approach for fabricating through-layer structures with high resolution. Without interlayer communication structures, fluid routing, control, and sample addressing become challenges when sample size becomes large.

Several prior fabrication approaches have been demonstrated to solve the issue of fabricating interlayer communication structures, but with different degrees of success. One simple method is the use of a multilevel mold with raised post structures. By spinning a thin, uncured PDMS layer on this mold, through-layer vias can be formed at locations with these raised posts [22]. This method, although simple, does not provide large area uniformity since it is sensitive to many parameters such as via height, membrane thickness, and density of vias. To prevent the formation of residual membranes at via locations, an approach utilizing pressure gas to blow off uncured PDMS at via locations has been demonstrated as well, but there are concerns regarding the throughput and uniformity across the chip.[23].

Another approach is to utilize a soft PDMS stamp to fabricate PDMS thin films with through-layer structures and stack them layer-by-layer [24]. A soft PDMS stamp ensures the removal of the interface residues between the stamp and the mold. This approach, however, introduces an edge protrusion issue near vias due to a deformed stamp in the molding process. These nonplanar features can accumulate and limit the number of layers that can be stacked

since bonding nonflat surfaces is challenging. For fine features such as narrow high-aspect-ratio structures, these protruding edges prohibit their bonding with hard substrates, and limit the structure resolution that can be fabricated. Another approach utilizing a hard glass stamp with the aid of amine surface treatment has also been demonstrated. The amine treatment can inhibit the polymerization process of a thin uncured PDMS layer adjacent to the stamp surface to remove the residual PDMS at through-layer regions [25, 26]. The diffusion-based polymerization inhibition process, however, limits the structure density and resolution of layer thickness. Another approach using CO₂ laser to directly ablate through a thin PDMS film is also demonstrated. However, this approach generates rough surfaces and non-vertical sidewalls [27].

Here, we demonstrate a hybrid stamp approach to solve the edge protrusion issue and provide a reliable method for fabricating high aspect ratio (HAR), high resolution PDMS 3D thin-film structures across a large area. HAR is defined as the ratio of structure height to width. In this approach, a PDMS stamp is embedded with a thin plastic plate underneath a chemically treated PDMS surface. This plastic plate increases the mechanical stiffness near the stamp surface to prevent severe deformation to eliminate the occurrence of protruding edges. A thin layer of elastic PDMS film on top of the plastic plate provides the required elasticity to ensure a complete removal of uncured PDMS residues at through-layer regions. Removing edge protrusion is a significant step. It permits the fabrication of high resolution, large area, high-aspect-ratio PDMS thin films with through-layer features to construct 3D microfluidic devices. Flat PDMS interfaces allow narrow HAR structures to be bonded reliably between hard substrates, on which high quality electronic, optical, and semiconductor devices are typically fabricated. This gives chip designers more flexibility in integrating heterogeneous materials, structures, devices, and systems on the same chip with more functional modules.

Fabrication of 3D Microfluidic Networks with a Hybrid Stamp

Fig. 1 shows the schematic of the process flow of fabricating 3D microfluidic structures using the hybrid stamp approach.

Step 1: Fabrication of master molds. It starts from fabricating SU-8 mold masters on silicon wafers using photolithography (Fig. 1(a)). A thin SU-8 layer is coated before the thick SU-8 mold to enhance the adhesion to the bulk silicon wafer. All masters need to be surface treated with trichloro (1H,1H,2H,2H-perfluorooctyl) silane (97%, Sigma-Aldrich, USA), also called PFOCTS, to facilitate later demolding. This surface treatment was carried out in a vacuum chamber at a pressure of -30 psi for 16 hours.

Step 2: Fabrication of hybrid stamps. It starts from preparing the Sylgard 184 silicone elastomer mixture (Dow Corning Corporation, Miland, USA). The ratio of Base : Curing agent is 10g : 1g. Few drops of this mixture are poured into a petri dish. A suitable size of polystyrene plastic plate is cut and pressed against the bottom of the petri dish under a pressure of 3 psi. A thin layer of polydimethylsiloxane (PDMS) with a thickness of roughly 30 μ m is formed between the petri dish and the plastic plate. Additional uncured PDMS is poured to fill up the petri dish, followed by a curing step at 60 $^{\circ}$ C in an oven for 12 hours. A hybrid stamp is formed when the plastic plate together with a thin PDMS layer on its surface is peeled off from the petri dish (Fig. 1(b)). The hybrid stamp is also surface treated with PFOCTS as in Step 1 for 6 hours. To fabricate PDMS thin film with through-layer structures, uncured PDMS is poured onto the master mold, pressed by the hybrid stamp under a pressure of 4psi, and cured at 50 $^{\circ}$ C in an oven for an hour.

Step 3: Demolding PDMS films from master mold. During the demolding process, the cured PDMS thin film has stronger adhesion to the hybrid stamp than to the master mold since more PFOCTS is coated on the master mold due to a longer treatment time (Fig. 1(c)).

Step 4: Transfer and stack PDMS thin films. Oxygen plasma treatment is performed on both the PDMS thin film on the hybrid stamp and the substrate to be bonded for two minutes. Alignment is performed under a microscope before bonding (Fig. 1(d)). The bonded set is baked in an oven at 60°C for 2 hours.

Step 5: Removing hybrid stamp. It starts from peeling off the bulk PDMS part on the plastic plate (Fig. 1(e)), followed by dissolving the polystyrene plastic plate in an acetone bath for 4 hours (Fig. 1(f)). This leaves a thin residual PDMS film on the substrate that can be easily peeled off from the device due to prior PFOCTS treatment (Fig. 1(g)) to finish the transferring and stacking process of a PDMS thin film with through-layer structures. This mechanically gentle releasing technique allows us to transfer PDMS thin film to fragile substrates, such as a glass cover slip, over a large area.

Step 6: Constructing multilayer 3D microfluidic devices. By repeating step 1-5, multilayer 3D PDMS structures with interlayer vias and high aspect ratio structures could be constructed and bonded between two hard substrates (Fig. 1(h)).

Results and Discussion

The purpose to utilize a hybrid stamp in the molding process is to remove the protruding edges of the molded PDMS structures. If the stamp is made purely of PDMS, the contact surface is relatively soft. When a pressure is applied on a stamp to clear PDMS residuals at through-layer regions, the stamp at contact regions deforms. Since uncured PDMS is solidified between a deformed stamp and a mold, protruding edges are formed and transferred to the molded structures. These non-flat surfaces inhibit follow-up bonding with other structures. This problem becomes severe when small features are transferred since the protruded edges can occupy a

significant area on these features. Tight contact required for good bonding between layers is not allowed. A similar deformation issue also occurs in the alternative approach of creating through-layer PDMS structures using a soft master mold and a hard stamp. In the case of a hard master mold and a hard stamp combination, the uncured PDMS residuals at the through-layer regions cannot be completely removed. The novelty of the plastic embedded hybrid stamp is to provide a stiff stamp to prevent deformation, while keeping a required elasticity at the contact interface to ensure a complete removal of uncured PDMS at through-layer regions. The plastic plate has a Young's module of $E=3.2\text{GPa}$, much larger than the PDMS Young's modulus ($E=0.6\text{MPa}$). Fig. 2(a,b) and (c,d) shows the degree of edge deformation of PDMS structures molded by a standard PDMS stamp and a hybrid stamp, respectively. In Fig. 2(d), an open microfluidic channel with HAR (5:1) PDMS walls is demonstrated. Fig. 3 shows a multilayer PDMS structure with pneumatically driven microvalves sandwiched between two hard, transparent, and electrically conductive ITO glass substrates. In addition, a $30\ \mu\text{m}$ thick PDMS membrane with a high-density array of HAR through-layer vias that are $6\ \mu\text{m}$ in diameter has also been successfully fabricated, as shown in Fig. 4. The pitch between vias is $100\ \mu\text{m}$. **Table 1** in supplemental material summarizes recent representative works on fabrication of 3D microfluidics structure. Parameters including lateral resolution, layer thickness resolution, hard substrate bonding ability, and HAR value are provided for comparison with the current work. The resolution and HAR value of our current approach is limited by the resolution of photolithography for making the master mold. To create a HAR structure with a lateral resolution of $6\ \mu\text{m}$, the maximum thickness we can achieve is $30\ \mu\text{m}$ due to the optical diffraction limit when patterning a thick photoresist.

High Aspect Ratio Deformable Membranes for 3D Dielectrophoresis Focusing

In addition to providing three-dimensional fluid routing, the ability to fabricate vertical, thin, HAR PDMS membranes and bond them with hard substrates allows the fabrication of deformable channels. This unique advantage promises novel functional devices not possible before, especially in fields such as electrokinetics, optofluidics, and inertial microfluidics, in which the channel cross-section profile plays a critical role in underlying device physics. For example, particle focusing equilibrium locations can change in a high-speed inertia flow when the channel deforms; and a curved and deformed channel can work as a tunable lens for light focusing and collection in optofluidics.

Here, we demonstrate a novel electrokinetics device that can achieve tunable 3D cell focusing in the center of a channel without sheath flows. Fig. 5(a,b) shows the schematic of such a device fabricated using the hybrid stamp approach. A single layer PDMS thin film with high aspect ratio (HAR=4) walls is bonded between two featureless ITO glass substrates. Fig. 5(c) shows the picture of a completed microfluidic device. By applying pressure to the two side channels, the middle channels can be deformed as shown in Fig. 5(b). Application of an electrical bias to the two featureless ITO electrodes causes electric field streamlines to be focused in the middle neck of the deformed channel, creating a highly non-uniform electric field distribution with the maximum field enhancement occurring in the center. (Fig. 5(d)).

Fig. 6(a), (b) show the microscope images of a channel with vertical sidewalls of 80 μm high and 20 μm thick before and after a pressure of 60psi is applied to the side channels, respectively. **Video 1** in supplemental material shows the tunable channel deformation when different pneumatic pressure values were applied to the side channel. An alternating current

(a.c.) signal is applied to the top and bottom ITO electrode to provide the electric field required for cell focusing using dielectrophoresis.

Dielectrophoresis (DEP) is a phenomenon in which a particle in a non-uniform electric field can experience an electrostatic force moving the particle towards stronger electric field regions if the particle is more polarizable than the medium, called positive DEP. A particle moves to weaker electric field regions if the particle is less polarizable than the medium, called negative DEP [28] [29] [30-33]. To migrate a particle in an electric field using dielectrophoresis, there must be electric field gradient. In a uniform electric field region, although particles are polarized, no net DEP forces can be induced for moving.

Fig. 6(c)(d) compares the simulated electric field distribution in a channel with and without deformation, respectively. Since the sidewalls can be continuously deformed to eventually contact each other and seal the gap, this device allows the tuning of the electric field strength in the middle of the channel by controlling the applied pressure in the side channels. The narrower the neck, the larger the electric field enhancement is generated in the neck. This allows the creation of strong electric field gradients for focusing small objects such as bacteria. Cells or particles experiencing positive DEP forces in the channel are attracted to the center of the channel, providing a continuous 3D sheathless cell focusing function for potential applications in microfluidic flow cytometers and cell sorters.

The performance of 3D DEP focusing on this deformable channel is tested using two types of cells, GFP-Hela with a diameter of 15 μ m and GFP-E. Coli with rod shape of 2 μ m long and 700 nm in diameter. Before pumping the sample into the device, GFP-Hela cells was suspended in an isotonic buffer consisting of 8.5% sucrose and 0.3% dextrose and with a conductivity of 10mS/m. GFP-E. Coli was suspended in a buffer solution of 10% sucrose in 20

mM HEPES and with a conductivity of 30mS/m. The sample was injected continuously into the microchannel by a syringe pump (kdScientific, 780100). A function generator (Agilent, 33220A) and power amplifier (ENI, Model 2100L) were used to provide the a.c. voltage source. The DEP response of the cells were monitored under an inverted fluorescence microscope (Carl Zeiss, Axio Observer.A1), and recorded by a CCD camera (Carl Zeiss, AxioCam MRm). For the HeLa-GFP focusing, the side channel was pressured at 35psi to create a 16 μ m wide gap, roughly the size of HeLa cells. When an a.c. signal (300kHz, 56.6V peak-to-peak) was applied, GFP-Hela cells were focused to the center of the channel (Fig. 7(b)), and remained focused in the downstream even at regions without deformed channels due to the laminar flow nature in microfluidics. To focus E. Coli, the sidewalls of the channel is further deformed to a smaller gap of only 3 μ m to create a stronger electric field strength and gradient for focusing these smaller objects. When there was no a.c. signal applied, GFP-E. Coli were randomly distributed across the channel (Fig. 7(c)). Under the application of an a.c. signal (5MHz, 56.6V peak-to-peak), positive DEP forces focused GFP-E. Coli to the center of the channel to form a single stream fluorescence trace as shown in Fig. 7(d), and **video 2** in supplemental material.

Conclusion

This paper demonstrates a new fabrication approach capable of manufacturing multilayer, 3D, HAR, open PDMS based microfluidic structures that can be bonded between hard substrates. This approach utilizes a hybrid stamp that consists of a plastic plate embedded right underneath a thin PDMS film to provide the required hardness for preventing severe stamp deformation during molding processes. A thin layer of PDMS film on the plastic plate provides local elasticity to ensure a complete removal of uncured residual PDMS in the through-layer regions. HAR PDMS structures fabricated by this method do not have protruding edges and offer flat

interfaces for multilayer stacking and bonding with hard substrates. Using this unique fabrication capability, we demonstrate deformable channel formed by sandwiching thin, vertical, HAR PDMS channel walls between two ITO substrates. These thin channel sidewalls can be continuously deformed under pressure to change the cross-section of a channel, a feature that may find many applications in fields such as optofluidics, inertial microfluidics, and electrokinetics that have channel profile sensitive physical phenomena. To demonstrate, we utilized this deformable channel structure to achieve single stream, 3D, sheathless focusing of mammalian cells as well as small bacteria.

Acknowledgement

This work is supported by NSF DBI 1256178, NSF ECCS1232279, and Cal. Cap. LLC through an industry research agreement.

References

1. Yeo, L.Y., et al., *Microfluidic Devices for Bioapplications*. Small, 2011. **7**(1): p. 12 - 48.
2. J. Shi, S.Y., S.-C. Steven Lin, X. Ding, I.-K. Chiang, K. Sharp, Tony J. Huang, *Three-dimensional continuous particle focusing in a microfluidic channel via standing surface acoustic waves (SSAW)*. Lab on a Chip, 2011. **11**: p. 2319-2324.
3. J. Shi, X.M., D. Ahmed, A. Colletti, Tony J. Huang, *Focusing microparticles in a microfluidic channel with standing surface acoustic waves (SSAW)*. Lab on a Chip, 2008. **8**: p. 221 - 223.
4. Y. Chen, A.A.N., Y. Zhao, P.-H. Huang, J. Phillip McCoy, Stewart J. Levine, L. Wang, Tony J. Huang, *Standing surface acoustic wave (SSAW)-based microfluidic cytometer*. Lab on a Chip, 2014. **14**: p. 916-923.
5. Chen, Y., et al., *3D pulsed laser-triggered high-speed microfluidic fluorescence-activated cell sorter*. Analyst, 2013. **138**: p. 7308-7315.
6. Fan, Y.J., et al., *Three dimensional microfluidics with embedded microball lenses for parallel and high throughput multicolor fluorescence detection*. BIOMICROFLUIDICS, 2013. **7**(4): p. 044121.
7. Huh, D., et al., *Reconstituting Organ-Level Lung Functions on a Chip*. Science, 2010. **328**(No. 5986): p. 1662 - 1668.
8. Jang, Y.-H., et al., *An integrated microfluidic device for two-dimensional combinatorial dilution*. Lab on a Chip, 2011. **11**(19): p. 3277 - 3286.

9. Kim, J., et al., *A programmable microfluidic cell array for combinatorial drug screening*. Lab on a Chip, 2012. **12**(10): p. 1813 - 1822.
10. Liu, M.C., D. Ho, and Y.-C. Tai, *Monolithic fabrication of three-dimensional microfluidic networks for constructing cell culture array with an integrated combinatorial mixer*. Sensors and Actuators B: Chemical, 2008. **129**(2): p. 826 - 833.
11. Liu, M.C. and Y.-C. Tai, *A 3-D microfluidic combinatorial cell array*. Biomedical Microdevices, 2011. **13**(1): p. 191 - 201.
12. Ostuni, E., et al., *Patterning Mammalian Cells Using Elastomeric Membranes*. Langmuir, 2000. **16**(20): p. 7811 - 7819.
13. Wang, Y., et al., *Capture and 3D culture of colonic crypts and colonoids in a microarray platform*. Lab on a Chip, 2013. **13**(23): p. 4625-4634.
14. Gregory, C.W., et al., *High yield fabrication of multilayer polydimethylsiloxane devices with freestanding micropillar arrays*. BIOMICROFLUIDICS, 2013. **7**(5): p. 0565503.
15. Brassard, D., et al., *3D thermoplastic elastomer microfluidic devices for biological probe immobilization*. Lab on a Chip, 2011. **11**(23): p. 4099-4107.
16. Agirregabiria, M., et al., *Fabrication of SU-8 multilayer microstructures based on successive CMOS compatible adhesive bonding and releasing steps*. Lab on a Chip, 2005. **5**: p. 545 - 552.
17. Patel, J.N., et al., *SU-8- and PDMS-based hybrid fabrication technology for combination of permanently bonded flexible and rigid features on a single device*. JOURNAL OF MICROMECHANICS AND MICROENGINEERING, 2013. **23**(6): p. 065029.
18. Patel, J.N., et al., *PDMS as a sacrificial substrate for SU-8-based biomedical and microfluidic applications*. JOURNAL OF MICROMECHANICS AND MICROENGINEERING, 2008. **18**: p. 095028.
19. Unger, M.A., et al., *Monolithic Microfabricated Valves and Pumps by Multilayer Soft Lithography*. Science, 2000. **288**(5463): p. 113 - 116.
20. Hong, J.W. and S.R. Quake, *Integrated nanoliter systems*. Nature Biotechnology, 2003. **21**: p. 1179 - 1183.
21. Thorsen, T., S.J. Maerkl, and S.R. Quake, *Microfluidic Large-Scale Integration*. Science, 2002. **298**(5593): p. 580-584.
22. Kartalov, E.P., et al., *Microfluidic vias enable nested bioarrays and autoregulatory devices in Newtonian fluids*. Proceedings of the National Academy of Sciences of the United States of America, 2006. **103**(33): p. 12280–12284.
23. Kang, J.H., E. Um, and J.-K. Park, *Fabrication of a poly(dimethylsiloxane) membrane with well-defined through-holes for three-dimensional microfluidic networks*. JOURNAL OF MICROMECHANICS AND MICROENGINEERING, 2009. **19**: p. 045027.
24. Zhang, M., et al., *A simple method for fabricating multi-layer PDMS structures for 3D microfluidic chips*. Lab on a Chip, 2010. **10**(9): p. 1199 - 1203.
25. Carlborg, C.F., et al., *A High-Yield Process for 3-D Large-Scale Integrated Microfluidic Networks in PDMS*. JOURNAL OF MICROELECTROMECHANICAL SYSTEMS, 2010. **19**(5): p. 1050 - 1057.
26. Karlsson, J.M., et al., *Fabrication and transfer of fragile 3D PDMS microstructures*. JOURNAL OF MICROMECHANICS AND MICROENGINEERING, 2012. **22**(8).
27. Li, M., et al., *A simple and cost-effective method for fabrication of integrated electronic-microfluidic devices using a laser-patterned PDMS layer*. Microfluidics and Nanofluidics, 2012. **12**(5): p. 751-760.
28. Khoshmanesh, K., et al., *Dielectrophoretic Platforms for Bio-microfluidic Systems*. Biosensors and Bioelectronics, 2011. **26**(5): p. 1800-1814.

29. Pethig, R., *Review Article—Dielectrophoresis: Status of the theory, technology, and applications*. BIOMICROFLUIDICS, 2010. **4**(2): p. 022811.
30. Barbulovic-Nad, I., et al., *DC-dielectrophoretic separation of microparticles using an oil droplet obstacle*. Lab on a Chip, 2006. **6**(2): p. 274-279.
31. Cummings, E.B. and A.K. Singh, *Dielectrophoresis in Microchips Containing Arrays of Insulating Posts : Theoretical and Experimental Results*. Analytical Chemistry, 2003. **75**(18): p. 4724-4731.
32. Kang, K.H., et al., *Continuous separation of microparticles by size with Direct current-dielectrophoresis*. Electrophoresis, 2006. **27**(3): p. 694-702.
33. Salmanzadeh, A., et al., *Isolation of prostate tumor initiating cells (TICs) through their dielectrophoretic signature*. Lab on a Chip, 2011. **12**(1): p. 182-189.

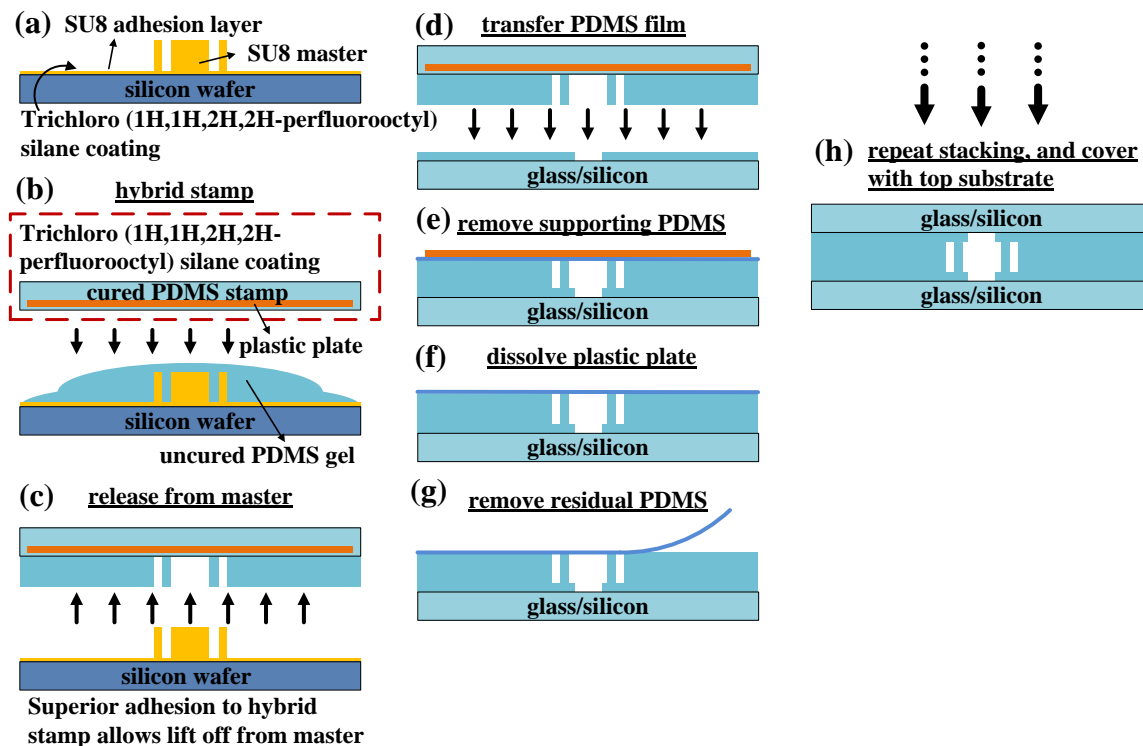


Fig. 1 Schematic of fabrication process flow using a plastic plate embedded hybrid stamp. (a) A SU8 master is treated with PFOCTS to facilitate later demolding. (b) Uncured PDMS mixture is poured on the master, and pressed against the hybrid stamp. (c) Due to less PFOCTS treatment on the hybrid stamp compared to the master, the casted PDMS film tends to adhere to the hybrid stamp and allows to be peeled off from the master. (d) The film is transferred and bonded by oxygen plasma treatment (e) Remove the support PDMS on the hybrid stamp. (f) Dissolve the polystyrene plastic plate in acetone. (g) Remove the residual PDMS thin film to complete the removal of a hybrid stamp. (h) The stacking process is repeated to complete the fabrication process, which includes bonding with a hard substrate.

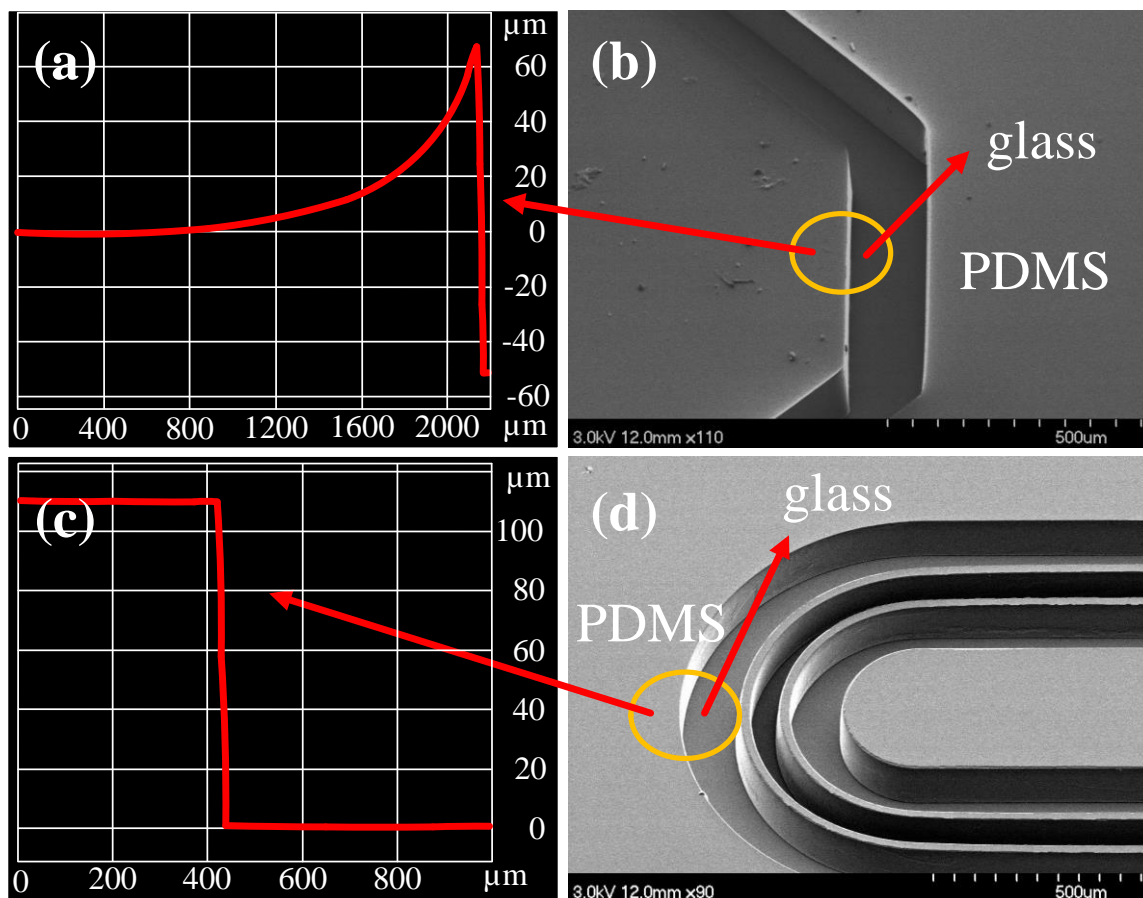


Fig. 2 (a, b) Edge protrusion issue near open structures of a PDMS thin film fabricated with a standard elastic PDMS stamp. This issue can be eliminated by using a plastic sheet embedded hybrid stamp in the molding process as shown in (c, d). Without the embedded plastic sheet, the contact surface is soft and results in protrusion edge around the channel. With the hybrid stamp, the contact surface is much more rigid to prevent the edge protrusion, and retains its ability to handle freestanding HAR sidewall structure.

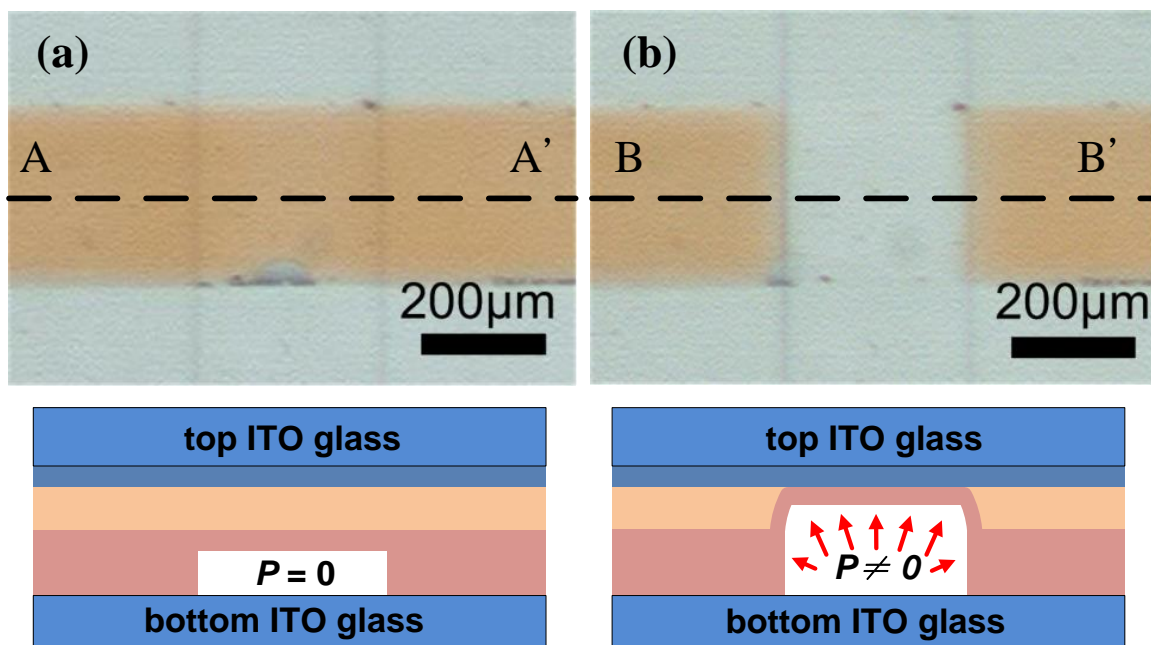


Fig. 3 Two layers of thin film PDMS structure with integrated pneumatic microvalve are bonded and sandwiched between two ITO coated glass substrates. (a) The top layer with fluidic channel is filled with dye liquid. The bottom layer is filled with uncolored DI water. The pneumatic pressure applied to the bottom channel $P=0$, which causes no valve membrane deformation. The subset shows the cross-sectional view along AA' line. (b) When a sufficient pneumatic pressure P is applied to the bottom channel, the valve membrane deforms and fully closed the top channel. The subset shows the cross-sectional view along BB' line.

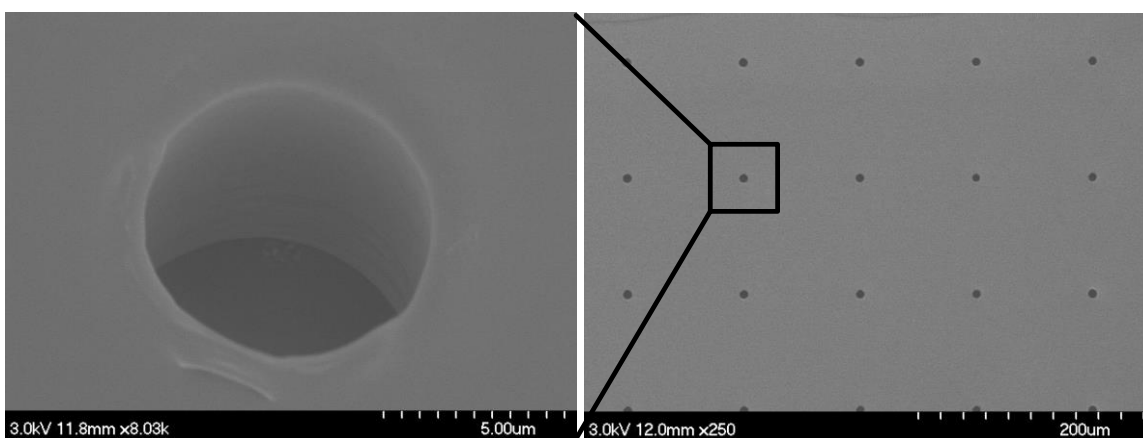


Fig. 4 SEM images of a 30 μm thick PDMS membrane with an array of 6 μm wide through-layer holes.

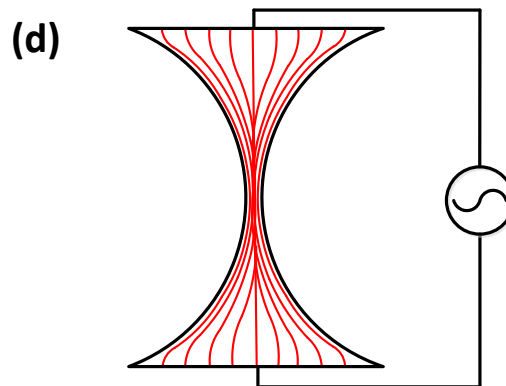
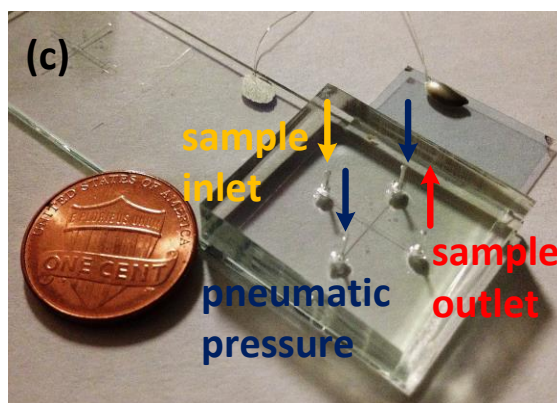
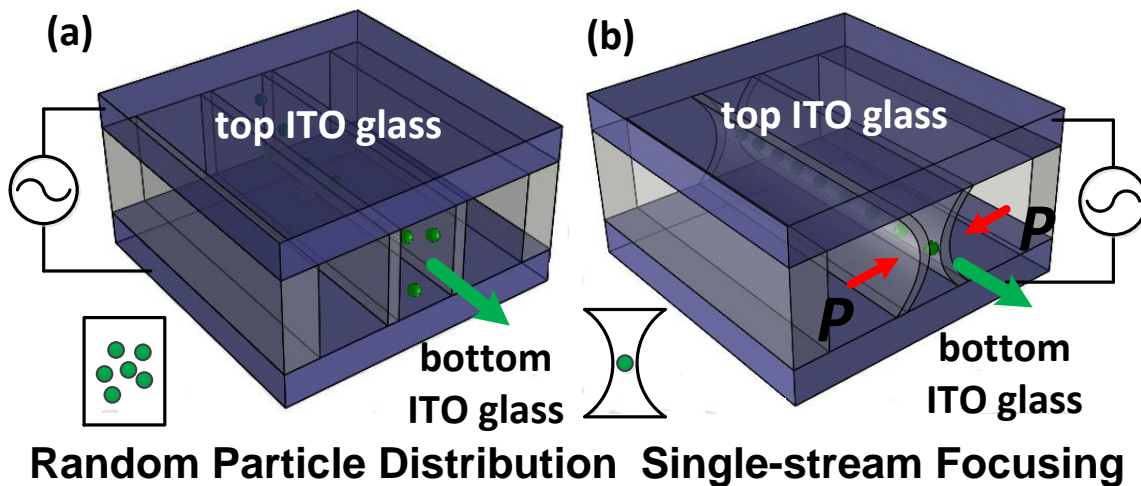


Fig. 5 Schematic of a tunable 3D DEP focusing device. (a) An open PDMS microchannel with thin, high-aspect-ratio sidewalls is sandwiched between two conductive indium tin oxide (ITO) coated glass substrates. An a.c. signal is applied between the top and bottom substrate. (b) When the channel sidewalls are pressurized, the channel deforms to form a narrow neck in the middle and focus the electric field lines. Positive DEP responding particles would migrate to the center of the channel where the maximum electric field occurs. (c) Photograph of a fabricated device. (d) A schematic showing crowding electric field streamlines in the neck of a deformed channel.

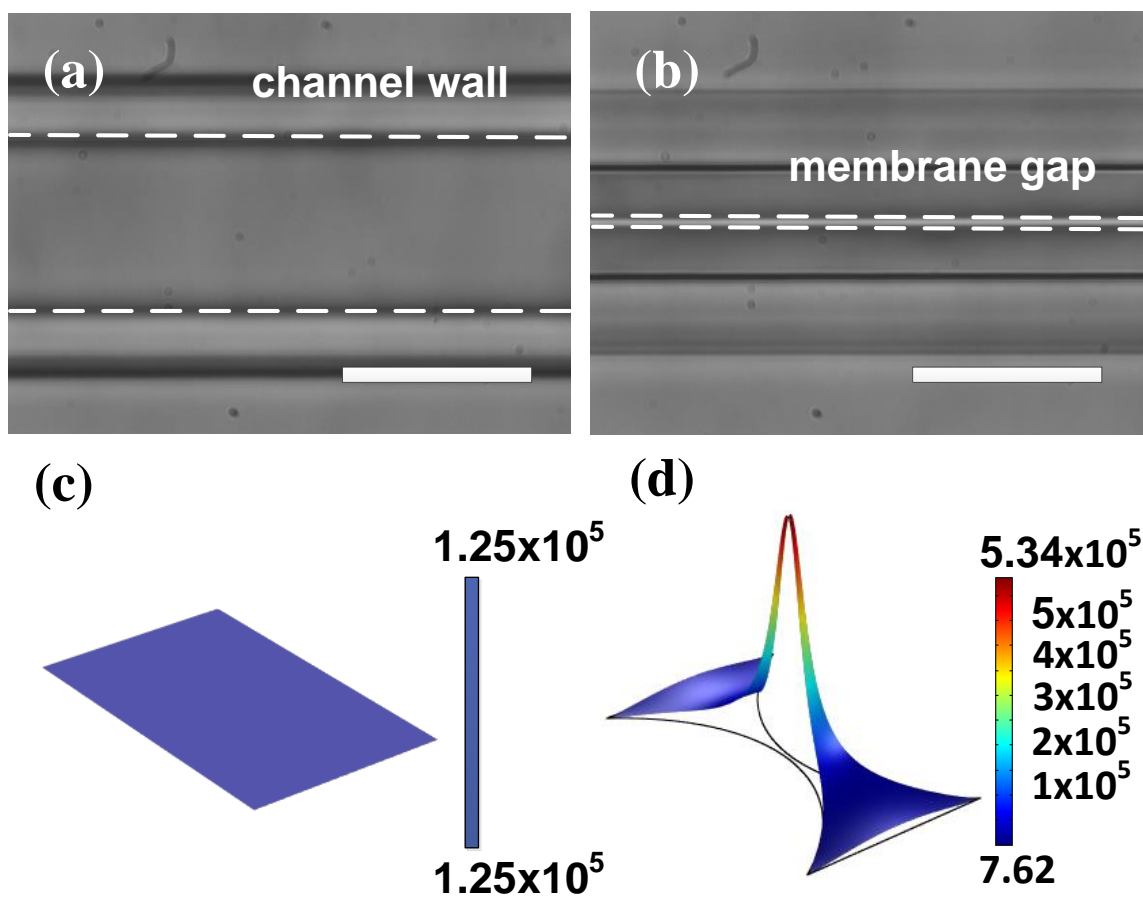


Fig. 6 (a) Microscopy images of a deformable microchannel with a dimension of $50\mu\text{m}$ in width, $80\mu\text{m}$ in height, and a sidewall thickness of $20\mu\text{m}$. (b) The channel sidewalls are under of pressure of 60psi . (c) Electric field distribution in a microchannel without deformation under an ac bias of 10V peak-to-peak at a frequency of 5MHz . (d) When the channel is deformed to form a neck that is only $0.5\mu\text{m}$ width, strong field enhancement is generated in the middle of this channel. Scale bar : $50\mu\text{m}$

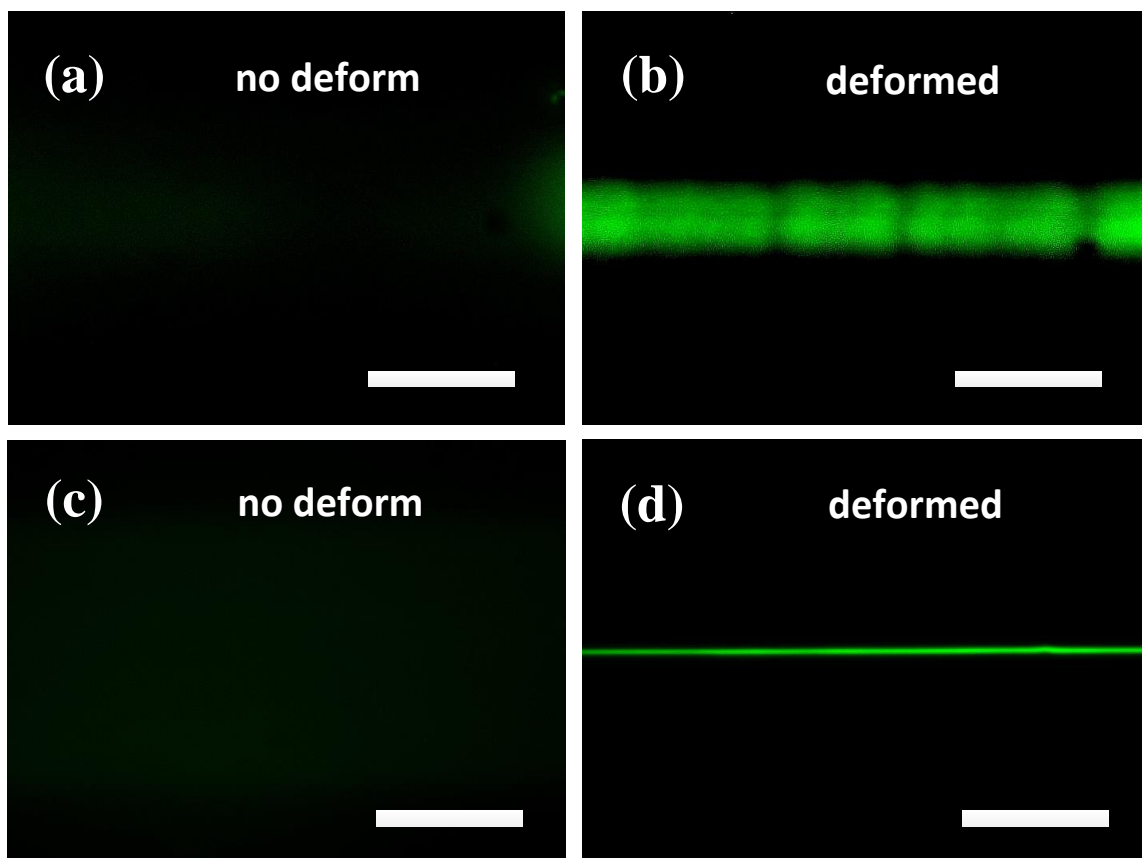


Fig. 7 The focused fluorescence traces of biological objects. All samples are suspended in media with conductivities ranging from 10 mS/m to 30 mS/m. An a.c. signal of 56.6V peak-to-peak with frequencies varying from 300 kHz to 5 MHz is applied. (a, b) compare the fluorescence traces of GFP-Hela (spherical shape, 15 μm in diameter) in a channel without and with sidewall deformation (35 psi) at an average flow speed of 17 cm/sec. The channel neck in (b) is 16 μm; (c, d) compare the traces of GFP-E. coli (rod-shape, 2 μm long and 700 nm wide) in a channel without and with sidewall deformation (60 psi) deformation at an average flow speed of 14 cm/sec. The channel neck in (d) is 3 μm. Scale bar : 25 μm